J Mater Sci (2009) 44:680–684
DOI 10.1007/s10853-008-3177-x

LETTER

Characterization of microstructural effects in a percussion laser-drilled powder metallurgy Ni-based superalloy

Jacquelynn K. M. Garofano · Harris L. Marcus · Mark Aindow

Received: 26 November 2008 / Accepted: 9 December 2008 / Published online: 24 December 2008

In the combustion zone of gas turbine engines for aircraft, it is essential to maintain a large temperature differential between the combustion gases and the Ni superalloy components so that fuel is used efficiently while avoiding degradation of the turbine blades, rotors, casings, etc. This is typically achieved using a combination of thermal barrier coatings (TBCs) and cooling holes [1–3]. In the latter case, air from the compressor section is forced through internal channels in the components and this emerges from arrays of fine (<500 μm in diameter) cooling holes, establishing a thin air layer between the combustion gases and the TBC. Current generation engines can contain in excess of 10^6 cooling holes and most of these are produced by electro-discharge machining (EDM) or laser drilling. The use of laser drilling is increasing because it enables holes to be drilled through components with TBCs (e.g. [4, 5]); this is a significant advantage over EDM where the holes must be formed in uncoated components and the subsequent application of a TBC can cause cooling-hole blockage.

Laser drilling of aerospace components is normally performed in percussion mode whereby the laser and component are stationary and a few short ($\approx$ms) intense laser pulses are used to produce the hole; each pulse melts and partially vaporizes the alloy, leading to ejection of the molten material and vapor through the irradiated surface [4–6]. Percussion laser drilling is usually preferred over both laser trepanning with a moving beam, which produces very high quality holes but with a longer cycle time, and single-shot drilling, which produces more debris and other artifacts (e.g. [5, 6]). The main metallurgical effects that can occur during percussion laser drilling are the formation of a recast layer and/or a heat-affected zone (HAZ) [5–8]. The recast layer is comprised of molten/vaporized metal that is not ejected from the hole by the vapor generated during the laser pulse but instead resolidifies on the side-wall of the hole [5, 6]. The HAZ consists of a region of the base metal surrounding the hole that has not melted during the drilling but has undergone microstructural changes due to the thermal history in a manner akin to the HAZs formed during laser welding and cladding (e.g. [9–12]). It is known that the recast and/or HAZ could lead to significant fatigue debits for laser-drilled components, and indeed this has been the motivation behind recent work on femtosecond ablative laser drilling in which recast and/or HAZ effects can be avoided [13, 14].

While there have been several parametric studies in which optical and scanning electron microscopy have been used to measure the extent of the recast and HAZ layers for such laser-drilled components (e.g. [15–18]), there has been little high-resolution characterization work to reveal the structures of these layers. In our work, we have used a variety of high-resolution microstructural characterization techniques to investigate the recast and HAZ structures for a variety of different Ni-based superalloys and preliminary data have been presented elsewhere [19]. The present paper describes a more detailed electron microscopy study of these structures for percussion laser-drilled samples of the powder metallurgy (P/M) superalloy IN100, which has a nominal composition of Ni–18.5Co–12.4Cr–5.0Al–4.3Ti–3.2Mo–0.8V–0.07C–0.06Zr–0.02B (all in wt%). This particular alloy was selected because in the P/M form it has a very uniform chemistry and a well-defined microstructure comprising a hierarchy of $L1_2$ γ' precipitates on different

J. K. M. Garofano · H. L. Marcus · M. Aindow (✉)
Department of Chemical Materials and Biomolecular Engineering, Materials Science and Engineering Program, Institute of Materials Science, University of Connecticut, 97 North Eagleville Road, Storrs, CT 06269-3136, USA
e-mail: m.aindow@uconn.edu

length scales (e.g. [20]). These include large (>1 μm) primary γ' grains, intermediate (100–300 nm) secondary γ' precipitates, and fine (<20 nm) tertiary γ' precipitates, with a total γ' volume fraction of $\approx 60\%$. Thus, this system should provide an extremely sensitive test for HAZ effects.

Plates of P/M IN100, 12 mm in thickness, were drilled using a Prima Convergent P50L Nd:YAG laser ($\lambda = 1.064$ μm) with an energy of 6 J pulse^{-1}, a pulse duration of 0.5 ms, and a pulse repetition frequency of 10 Hz. Pressurized air was used as an assist gas in the drilling process. We note that these are typical conditions for the percussion laser drilling of Ni-based superalloy aerospace components with Nd:YAG lasers. All of the data presented here were obtained from a single plate in which a 5 × 5 array of holes normal to the surface was drilled to partial penetration by controlling the number of pulses (four per hole giving a hole depth of ≈ 4 mm). The plate was sectioned parallel to the beam direction to reveal the sidewalls of the laser-drilled hole (Fig. 1). The sections were ground and then polished with diamond suspensions before etching using waterless Kalling's reagent followed by glyceregia (15 s) to reveal the γ' phase clearly [21]. The etched sections were examined using secondary electron (SE) imaging in a JEOL 6335F field emission scanning electron microscope (FESEM) equipped with a Thermo Noran System Six energy dispersive X-ray spectrometer (EDXS).

Thin foils for transmission electron microscopy (TEM) were prepared by electropolishing and focused ion-beam (FIB) milling. Foils from the base metal and from the recast layer in plan-view were prepared by electropolishing to perforation in a Struers Tenupol 5 twin-jet apparatus using a solution of 150 mL perchloric acid and 900 mL ethanol at −40 °C at an applied voltage of 20.5 V. For plan-view foils from the recast layer, the sidewall of the laser-drilled hole was covered with an acid-resistant varnish (Microshield^{TM}) so that the disc was thinned to perforation from the base metal side. Cross-sectional foils through the recast layer were prepared using FEI Strata 235 and Nova Nanolab 600i dual-beam FIBs. The specimens were examined in Philips EM-420 and FEI Tecnai T12 TEMs operating at an accelerating voltage of 120 kV.

All of the sectioned holes were found to exhibit similar features with uniform recast layers ≈ 10 μm in thickness on the sidewalls and a thicker (up to 25 μm) resolidified layer in the bottom of the hole. We note that the sidewall recast layers consisted of a series of sub-layers, one for each of the laser pulses (Fig. 1e). Figure 2 shows a SE FESEM image obtained from the interface between the base metal and the resolidified layer at the bottom of one hole. There is a clear difference between the microstructures on either side of the interface and the transition is very abrupt. The base metal microstructure corresponds to

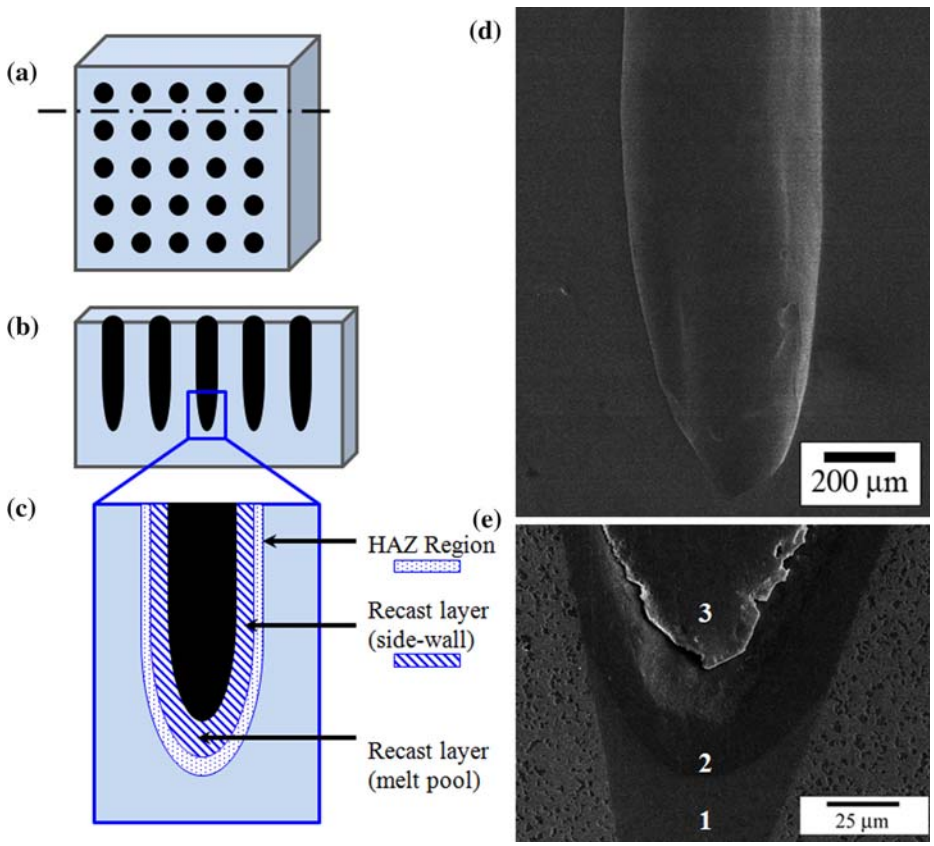

Fig. 1 **a–c** Schematic diagrams of the sample geometries: **a** arrangement of holes on the sample surface; **b** cross-sectional through a row of holes; **c** detail from **b** showing the recast layer in the sidewall and melt pool, together with the region in which a HAZ would form. **d–e** SE SEM images: **d** cross-section through the lower half of a hole; **e** detail from a hole angle-polished to reveal the sub-layers in the recast

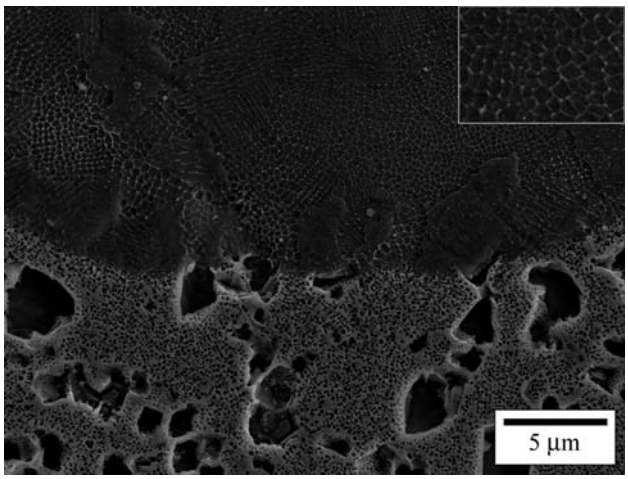

Fig. 2 SE SEM micrograph from a cross-sectional sample showing the boundary between the recast and base metal at the bottom of the melt pool. The inset is an enlargement from the recast showing the cellular microstructure in this layer

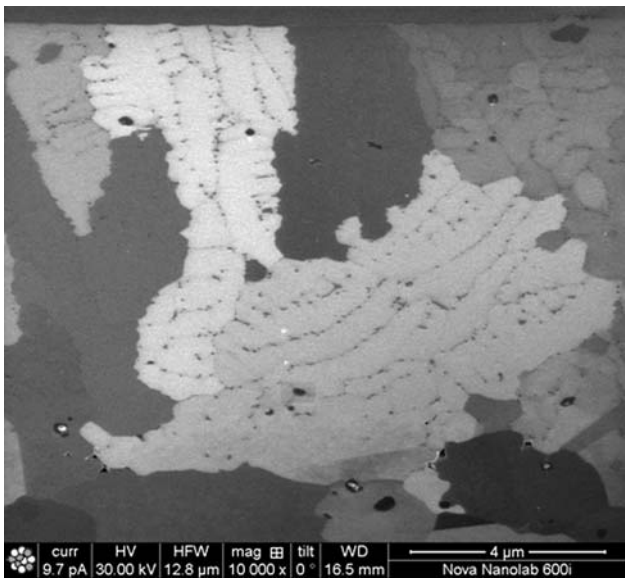

Fig. 3 SE ion beam image from a cross-sectional sample showing the dendritic character of the microstructure within the recast layer

that expected for P/M IN100 (e.g. [20]) and indeed there were no discernible differences between the microstructures of the base metal in such regions and those well away from the hole. Careful measurements of the primary and secondary γ' phases along probe lines parallel to the interface revealed no change in the sizes of these features with distance from the interface. Moreover, the EDXS data revealed no differences in the base metal chemistry as the interface was approached. Similarly, no changes in the base metal microstructure or chemistry were noted at the interfaces with the recast layer on the sidewalls. Thus, there is no measurable metallurgical HAZ in this system under these processing conditions.

The EDXS data revealed no significant differences between the chemistry of the base metal and that of the recast layer but the microstructures are very different; the recast layer exhibits a "cellular" contrast in the SE FESEM images (Fig. 2 and enlarged region inset) consisting of dark cells $\approx$300–500 nm in diameter delineated by bright (i.e. raised) boundaries. These cells are arranged into colonies $\approx$2–10 µm in diameter within which the cells are aligned in rows/arrays. The origins of this unusual contrast are suggested by SE ion beam images obtained from the walls of trenches cut during the FIB preparation of cross-sectional TEM foils from the recast layer. One example is shown in Fig. 3. Such images exhibit uniform intensity within the cellular colonies but very strong contrast between them. Such contrast is usually associated with changes in SE emission due to variations in the channeling of the Ga^+ ion beam with crystal orientation. Thus, the contrast is consistent with a dendritic-type structure wherein each colony corresponds to a single crystal orientation and each cell is a section through a dendrite arm.

The details of these structures were revealed more clearly in data obtained from the TEM foils (e.g. Fig. 4). A bright field (BF) image showing a typical region from the base metal is shown in Fig. 4a. This region contains γ and primary γ' grains with secondary γ' precipitates within the γ grains. The corresponding $[1\bar{1}0]$ zone axis selected area diffraction pattern (SADP) from a single γ grain is shown in Fig. 4b and this contains the 100- and 110-type $L1_2$ superlattice maxima that one would expect for a grain containing coherent secondary γ' precipitates. A BF image showing a typical region from the recast layer in the sidewall of a hole is shown in Fig. 4c. The overall morphology of the microstructure is very similar to that observed in SE FESEM images, except that the cell boundaries are dissolved preferentially by the electropolishing solution giving grooves rather than ridges at these locations. All of the SADPs such as Fig. 4d obtained from groups of cells corresponded to those expected for FCC crystals, and there was no evidence for $L1_2$ ordering. This is consistent with the colonies being dendrites of supersaturated γ phase as suggested by the SE FIB images.

No changes in structure or defect content were detected between the interior of the cells and the boundaries, but the EDXS data did reveal subtle compositional variations. Measurements were taken from 20 locations and the EDXS data were quantified using the overall alloy/recast chemistry as a standard. The mean composition (in wt%) measured at the centers of the cells was Ni–18.80Co–12.32Cr–5.16Al–3.54Ti–3.06Mo–0.86V, as compared to Ni–18.36Co–12.36Cr–5.52Al–4.03Ti–3.16Mo–0.89V at the cell boundaries. The differences in the Co, Cr, Mo, and V concentrations fall within the experimental scatter but

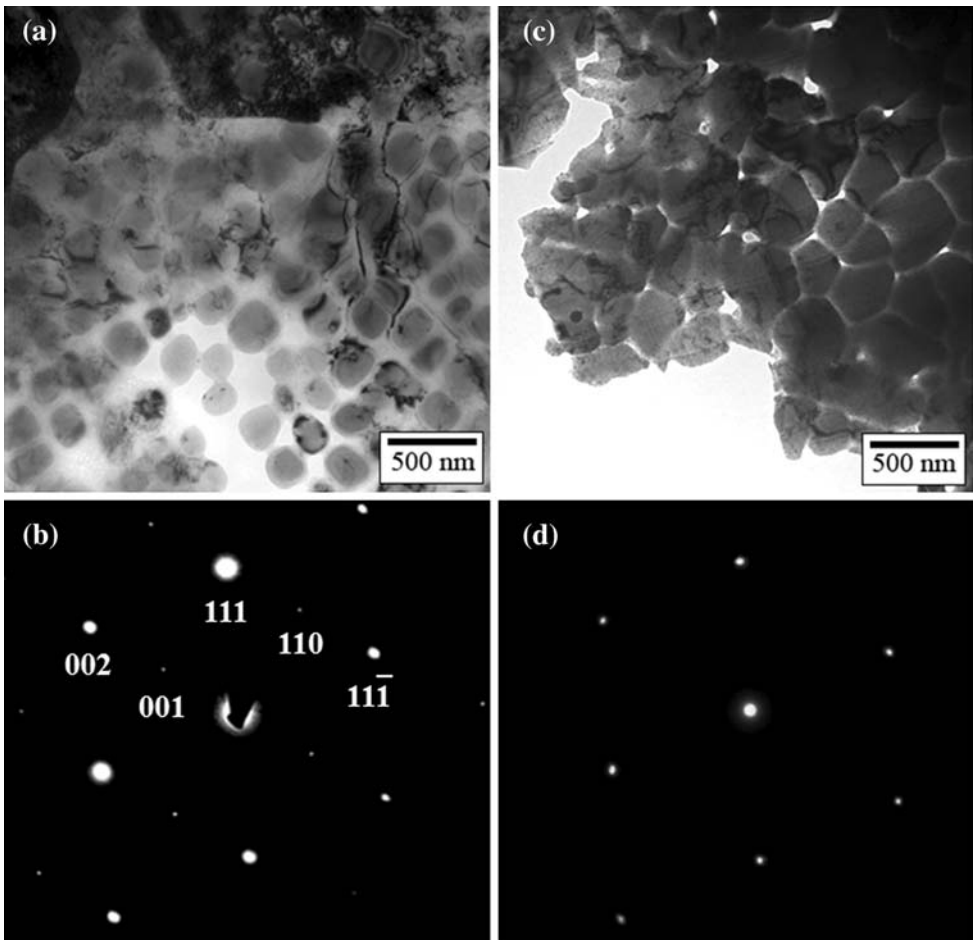

Fig. 4 TEM data (BF images and SADPs) obtained from electro-polished foils of: **a**, **b** base metal away from the drilled holes; **c**, **d** recast layer in plan-view with the foil plane parallel to the base metal/recast interface

the proportional change in the Al and Ti contents is larger and this enrichment was consistent for all locations. We note that these data may be an underestimate of the degree of the enrichment due to contributions from the surrounding cells when measuring the composition of the thin ($\approx$20 nm) cell boundary layers. Thus, the cellular appearance of the recast in both FESEM and TEM images probably arises due to differences in the etching and electro-polishing behavior due to dendritic microsegregation of Al and Ti.

Both the absence of any HAZ in these samples and the complete suppression of γ' precipitation in the recast layer are remarkable. In both cases, this is presumably due to the very short thermal transient giving insufficient time for the anticipated microstructural changes. The total processing time for each of the holes drilled in this study is less than 0.4 s and the volume of the recast layer on the sidewalls is less than 10% of the hole volume (i.e. over 90% of the molten/vaporized material is ejected from the hole). The presence of distinct sub-layers within the recast layer indicates that the redeposited material from one pulse has solidified completely before the arrival of the material from the next pulse; since the pulses are separated by 0.1 s, we estimate that the cooling rate for the molten/vaporized material depositing on the sidewalls is well in excess of 10^4 °C/s. The microsegregation of Al and Ti to the cell boundaries in the recast implies that the limited diffusion of the other transition metal species may be what prevents the precipitation of γ' phase. We note that partition coefficient for Cr is particularly large in this system ($P > 5$, e.g. [20]) and so this may be the controlling factor, although it is not clear why the diffusion of Cr should be more limited than that for Ti in this system. Similar factors could also be responsible for the absence of a HAZ in this case and indeed the same argument should hold for other superalloys, i.e. one might not expect the formation of a HAZ in Ni-based superalloys percussion laser-drilled under such conditions.

Acknowledgements The authors would like to thank Robin Bright (University of Connecticut) and Dr. Paul Denney of the Connecticut Center for Advanced Technology (CCAT) for helpful discussions, Robert Wright of CCAT for assistance with producing the laser-drilled samples, and Pal O. Pedersen of FEI Company and Dr. Kai Song of Lehigh University for assistance with FIB sectioning. This material is based on research sponsored by CCAT's National Center for Aerospace Leadership through Grant/Cooperative Agreement Number FA9550-06-1-0397 with the Air Force Office of Scientific

Research. The U.S. government is authorized to reproduce and distribute reprints for Governmental purposes notwithstanding any copyright notation thereon. The views and conclusions contained herein are those of the authors and should not be interpreted as necessarily representing the official policies or endorsements, either expressed or implied, of the Air Force Research Laboratory or the U.S. government.

References

1. Padture NP, Gell M, Jordan EH (2002) Science 296:280
2. Bunker RS (2005) ASME J Heat Transf 127:441
3. Bunker RS (2007) ASME J Turbomach 129:193
4. McNally CA, Folkes J, Pashby IR (2004) Mater Sci Technol 20:805
5. Dahotre NB, Harimkar SP (2008) Laser fabrication and machining of materials. Springer
6. Dubey AK, Yadava V (2008) Int J Mach Tool Manuf 48:609
7. Pandey ND, Shan HS, Mohandas T (2006) Mater Manuf Process 21:383
8. Bandyopadhyay S, Sarin Sundar JK, Sundararajan G, Joshi SV (2002) J Mater Process Technol 127:83
9. Steen WM (1991) Laser materials processing. Springer
10. Lemmen HJK, Sudmeijer KJ, Richardson IM, van der Zwaag S (2007) J Mater Sci 42:5286. doi:10.1007/s10853-006-0168-7
11. Mumtaz KA, Hopkinson N (2007) J Mater Sci 42:7647. doi:10.1007/s10853-007-1661-3
12. Xu PQ, Gong HY, Xu GX et al (2008) J Mater Sci 43:1559. doi:10.1007/s10853-007-2339-6
13. Feng Q, Picard YN, Liu H, Yalisove SM, Mourou G, Pollock TM (2005) Scr Mater 53:511
14. Feng Q, Picard YN, McDonald JP, Van Rompay PA, Yalisove SM, Pollock TM (2006) Mater Sci Eng A 430:203
15. Thawari G, Sarin Sundar JK, Sundararajan G, Joshi SV (2005) J Mater Process Technol 170:229
16. Sezer HK, Li L, Schmidt M, Pinkerton AJ, Anderson B, Williams P (2006) Int J Mach Tool Manuf 46:1972
17. Pandey ND, Shan HS, Bharti A (2006) Int J Adv Manuf Technol 28:863
18. Bright R, Jacobs P, Aindow M, Marcus HL (2007) Proceedings of ICALEO 2007, p 1201
19. Garofano JKM, Marcus HL, Aindow M (2008) Microsc Microanal 14(S2):558
20. Wusatowska-Sarnek AM, Ghosh G, Olson GB, Blackburn MJ, Aindow M (2003) J Mater Res 18:2653
21. Wusatowska-Sarnek AM, Blackburn MJ, Aindow M (2003) Mater Sci Eng A 360:390